A Journal of the Gesellschaft Deutscher Chemiker

Angewandte International Edition GDCh Chemie

www.angewandte.org

Accepted Article

Title: Titanium-Oxo Cluster Assisted Fabrication of a Defect-Rich Ti-MOF Membrane Showing Versatile Gas-Separation Performance

Authors: Chen Wang, Yanwei Sun, Libo Li, Rajamani Krishna, Taotao Ji, Sixing Chen, Jiahui Yan, and Yi Liu

To be cited as: *Angew. Chem. Int. Ed.* **2022**, e202203663

Link to VoR: https://doi.org/10.1002/anie.202203663

WILEY-VCH

10.1002/anie.202203663

WILEY-VCH

RESEARCH ARTICLE

Titanium-Oxo Cluster Assisted Fabrication of a Defect-Rich Ti-MOF Membrane Showing Versatile Gas-Separation Performance

Chen Wang,[a] Yanwei Sun,[a] Libo Li,[b] Rajamani Krishna,[c] Taotao Ji,[a] Sixing Chen,[a] Jiahui Yan,[a] Yi Liu*[a],[d]

[a] C. Wang, Dr. Y. Sun, T. Ji, S. Chen, J. Yan, Prof. Y. Liu
School of Chemical Engineering, State Key Laboratory of Fine Chemicals
Dalian University of Technology
Linggong Road 2, Ganjingzi District, Dalian 116024 (China)
E-mail: diligenliu@dlut.edu.cn
[b] Prof. L. Li
College of Chemistry and Chemical Engineering, Shanxi Key Laboratory of Gas Energy Efficient and Clean Utilization
Taiyuan University of Technology
Taiyuan 030024 (China)
[c] Prof. R. Krishna
Van 't Hoff Institute for Molecular Sciences
University of Amsterdam, Science Park 904
1098 XH Amsterdam, The Netherlands
[d] Prof. Y. Liu
Dalian Key Laboratory of Membrane Materials and Membrane Processes
Dalian University of Technology
Linggong Road 2, Ganjingzi District, Dalian 116024 (China)

Supporting information for this article is given via a link at the end of the document.

Abstract: Although having shown great promise for efficient gas separation, relevant study on Ti-MOF membranes remains very scarce, owing to limited Ti source types and uncertain factors which dominate the separation properties. In this work, we pioneered the use of $Ti_8(\mu_2\text{-}O)_8(OOCC_6H_5)_{16}$ cluster as Ti source of MIL-125 membranes, which led to lower reaction temperature and higher missing-linker number within the framework and therefore, enhanced CO_2/N_2 adsorption selectivity. The MIL-125 membrane prepared by combining single-mode microwave heating with tertiary growth displayed an ideal CO_2/N_2 selectivity of 38.7, which ranked the highest among all pristine pure MOF membranes measured under comparable conditions. In addition, the ideal H_2/N_2 and H_2/CH_4 selectivity was as high as 64.9 and 40.7, thus showing great promise for versatile utility in gas separation.

Introduction

As an alternative to traditional energy-intensive gas separation approaches like cryogenic distillation, liquid absorption and adsorption, membrane-based gas separation has shown remarkable advantages in terms of low energy consumption, easy operation, eco-friendship and small footprint.[1] Among various materials, metal−organic framework (MOF) has unique advantages in terms of tailorable pore aperture, adjustable functionality, and high surface areas. In particular, Ti-MOF has been considered a superb membrane material, owing to its excellent stability, appropriate pore size and unique adsorption behavior. MIL-125, which is representative of Ti-MOF materials, has a 3D framework with two kinds of cages (6.1 Å and 12.6 Å) and is accessible through the 5–7 Å microporous aperture. It consists of eight cyclic octamers of edge- and corner-sharing $[TiO_5(OH)]$ octahedra $Ti_8(\mu_2\text{-}O)_8(\mu_2\text{-}OH)_4$ nodes connected by 12 of 1,4-Benzene dicarboxylate (BDC) linkers.[2] Not only the relatively large pore size of MIL-125 warrants the high diffusivity of smaller-sized gases, but also its textural and functional properties can be tailored for specific gases adsorption.[3] Caro et al.[4] first prepared NH_2-MIL-125(Ti) membranes showing decent H_2/CO_2 selectivity (~8) by secondary growth. More recently, we synthesized highly c-oriented ultrathin NH_2-MIL-125(Ti) membranes showing significantly enhanced H_2/CO_2 selectivity (24.8).[5] Nevertheless, in comparison with some extensively studied MOF (like ZIF-8, HKUST-1 and UiO-66) membranes, relevant studies on polycrystalline Ti-MOF membranes remained scarce,[5] which could be, at least partially, attributed to limited types of titanium sources. For instance, titanium isopropoxide (TPOT) has been commonly employed as titanium source of Ti-MOF. However, it suffered from fast hydrolysis even under transient exposure to moisture in the air, resulting in uncontrollable nucleation and growth rates during Ti-MOF membrane formation.[6] Alternatively, the use of layered TiS_2 as titanium source enabled better control of nucleation and growth rates of Ti-MOF membranes so that their mesoscopic structures (e.g., preferred orientation, membrane thickness, and grain boundary defects) could be precisely tuned. Nevertheless, it remained impractical to further tailor their microscopic structures (e.g., missing-linker defects, pore aperture, and pore size distribution) which in turn, may exert more profound effect on the separation performance.

Previous studies indicated that missing-linker defects exerted a significant influence on the separation performance of MOF membranes. For instance, Zhong et al.[7] reported that diethanolamine-modified ZIF-8 membranes with abundant open metal sites displayed high C_3H_6/C_3H_8 selectivity. Park et al.[8] reported that defect-engineered UiO-66-incorporated mixed-matrix membranes exhibited exceptional C_3H_6 permeability and C_3H_6/C_3H_8 selectivity, owing to increased porosity and open metal sites caused by missing-linker defects in UiO-66 nanofillers. Very recently, we prepared highly defective UiO-66 membranes showing superior CO_2/N_2 separation performance through combining ZrS_2 source with tertiary growth.[9] Inspired by the

10.1002/anie.202203663

above achievements, herein we are dedicated to preparing high-performance Ti-MOF membranes through precisely tuning missing-linker defects in the framework.

Titanium-oxo cluster, which represents a member of tetravalent-transition-metal-oxo cluster family, consists of inorganic metal-oxide Ti-O-Ti cores capped with charge-compensating anions or -OH/-OH_2 pairs.[10] Decent coordinative interaction between cluster cores and charge-compensating anions renders titanium-oxo cluster the ideal metal source of Ti-MOF membranes since not only the activation energy for the formation of Ti-MOF can be significantly reduced via preorganization of cluster cores in the precursor solution which results in milder conditions for the growth of well-intergrown Ti-MOF membranes, but also missing-linker defects in the framework can be precisely tuned through manipulation of linker exchange rates which may have a positive effect on the separation performance. Park et al.[11] prepared DGIST-1 exhibiting excellent photocatalytic activity by employing $Ti_6O_6(OiPr)_6$(t-BA)$_6$ cluster as titanium source, which led to not only a higher degree of crystallinity but also increased accessible surface areas. Serre et al.[12] reported that the chemical environment and functionality of MIP-207 could be easily tuned through facile linker exchange with preformed $Ti_8(\mu_2\text{-}O)_8$(acetate)$_{12}$(formate)$_4$ (Ti_8AF) cluster. Compared with conventional TPOT, using Ti_8AF cluster source led to the formation of MIP-207 particles with not only superior CO_2/N_2 adsorption selectivity but also reduced synthesis duration. Very recently, Zhang et al.[3a] synthesized FIR-125 containing $Ti_8(\mu_2\text{-}O)_8$ nodes by employing titanium-oxo cluster as titanium source, which not only allowed easy tunning of the grain size but also gave rise to enhanced gas adsorption capacity. It should be noted that, although titanium-oxo cluster had proven to be ideal titanium source of Ti-MOF in powder form, there is still no report on the preparation of Ti-MOF membranes with titanium-oxo cluster source. Motivated by potential benefits derived from the titanium-oxo cluster, herein we pioneered the use of titanium-oxo cluster source for preparing high-performance Ti-MOF membrane.

MIL-125 has shown great promise for the application as gas adsorbents, smart photonic devices, and photocatalysis.[2a, 13] Its potential as high-performance separation membranes, however, has not been fully explored yet. As a new member of titanium-oxo cluster family, $Ti_8O_8(OOCR)_{16}$ [R=C_6H_5] (Ti_8Ph), which consists of eight [TiO_6] octahedra ring linked by six μ_2- and two μ_3-O bridges,[14] possesses a similar structure as the $Ti_8(\mu_2\text{-}O)_8(\mu_2\text{-}OH)_4$ node in MIL-125 framework, thereby making it attractive alternative to common titanium sources. Additionally, our recent study indicated that compared with conventional heating methods, using single-mode microwave heating enabled better control of the microstructure of NH_2-MIL-125 (Ti) membranes, owing to a higher microwave field intensity and uniformity.[5] In the present work, with Ti_8Ph cluster as titanium source, highly defective MIL-125 membrane was prepared through combing single-mode microwave heating with tertiary growth (**Figure 1**). On the one hand, our research indicated that carrying out the reaction at lower temperatures enabled increasing missing-linker defects within MIL-125 framework, which warranted high-affinity interactions with CO_2 molecules at room temperature, thereby leading to high adsorption selectivity (14.3) as evidenced by the IAST model; on the other hand, relatively large pore size of MIL-125 warranted high diffusivity of smaller-sized gases through the membrane. As a result, not only the ideal CO_2/N_2 selectivity ranked the highest among all polycrystalline MOF membranes measured under similar conditions, but also the Robeson Upper Bound 2008 was overcome for versatile gas pairs. Most importantly, we found that only by using Ti_8Ph cluster source could high-performance MIL-125 membranes be prepared. It is expected that this metal-oxo cluster-based protocol could bring new insights into diverse high-performance MOF membrane preparations.

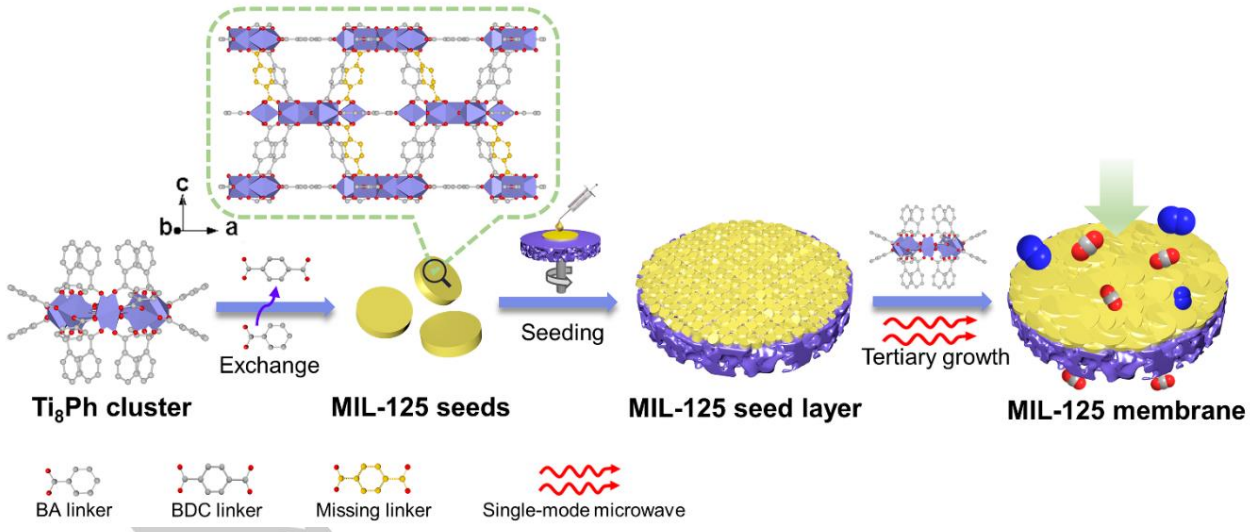

Figure 1. Schematic illustration of the preparation of defective MIL-125 membrane with Ti_8Ph cluster source through combing single-mode microwave heating with tertiary growth (BA: benzoic acid; BDC: terephthalic acid).

Results and Discussion

Our first step involves the synthesis of Ti_8Ph cluster according to a previous procedure with slight modification.[14] Relevant SEM images indicated that obtained products exhibited a well-defined needle shape (**Figure 2a**). The corresponding XRD pattern

10.1002/anie.202203663

coincided well with that of standard Ti_8Ph phase, implying that a pure Ti_8Ph cluster phase had been formed (**Figure 2b**).
Subsequently, two kinds of MIL-125 powders were prepared using Ti_8Ph cluster and TPOT as titanium sources, respectively. Our results indicated that uniform MIL-125 powders with an average size of 240 nm (**Figure 2c, d** and **Figure S1**) could be obtained by conducting linker exchange reaction between Ti_8Ph cluster and BDC linkers at temperature as low as 100 °C (denoted as MIL-125 (Ti_8Ph, 100 °C)). In contrast, the threshold temperature required for full conversion of TPOT to MIL-125 was 150 °C (denoted as MIL-125 (TPOT, 150 °C)) (**Figure S2**), indicating that using Ti_8Ph cluster source significantly lowered the activation energy required for MIL-125 formation.

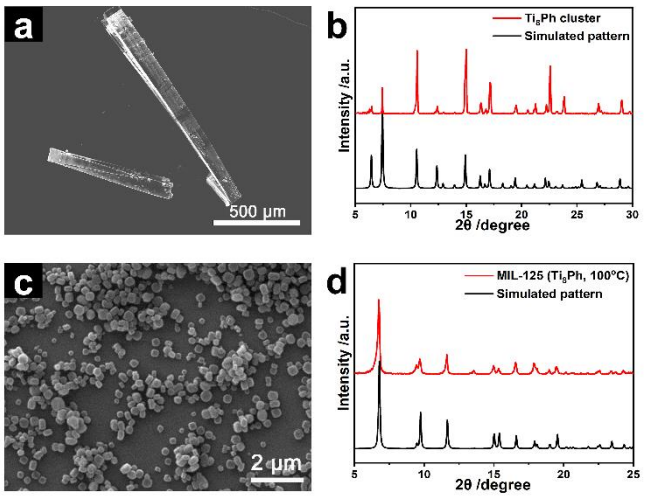

Figure 2. (a) SEM image of Ti_8Ph cluster. (b) XRD patterns of prepared Ti_8Ph cluster and simulated Ti_8Ph cluster. (c) SEM image of MIL-125. (d) XRD patterns of prepared MIL-125 (Ti_8Ph, 100 °C) and simulated MIL-125.

Considering the potential impact of missing-linker defects on the separation performance of MIL-125 membranes, herein the missing-linker number, which was widely used for quantitative evaluation of missing-linker defects, of the above MIL-125 powders was determined by TG analysis (shown in **Figure 3a**). According to the method proposed by Lillerud et al.[15], the missing-linker number per $Ti_8(\mu_2\text{-}O)_8(\mu_2\text{-}OH)_4$ node in the framework of MIL-125 (Ti_8Ph, 100 °C) reached 2.2, which was 5.5 times higher than MIL-125 (TPOT, 150 °C), implying that employing Ti_8Ph cluster source resulted in a significant increase in missing-linker number. In the next step, textural properties of the above MIL-125 powders were studied further. As shown in **Figure S3a**, N_2 adsorption/desorption isotherms revealed that MIL-125 (Ti_8Ph, 100 °C) exhibited a typical type I isotherm with BET surface area of 1453 $m^2 \cdot g^{-1}$, pore volume of 0.69 $cm^3 \cdot g^{-1}$, and pore size centering at 0.63 nm, which were all considerably higher than those of MIL-125 (TPOT, 150 °C) (1286.6 $m^2 \cdot g^{-1}$, 0.60 $cm^3 \cdot g^{-1}$, and 0.62 nm, respectively). Moreover, the CO_2 adsorption capacity of MIL-125 (Ti_8Ph, 100 °C) (103.42 $m^3 \cdot g^{-1}$) measured under ambient conditions was much higher than that of MIL-125 (TPOT, 150 °C) (53.05 $m^3 \cdot g^{-1}$) while maintaining similar N_2 adsorption capacity (**Figure S3b**). Much higher adsorption capacity of CO_2 than that of N_2 can be attributed to preferential adsorption of CO_2 on coordinatively unsaturated open metal sites in MIL-125 framework.[16] Moreover, CO_2/N_2 ideal adsorbed solution theory (IAST) selectivity of the above MIL-125 powders was calculated according to CO_2 and N_2 adsorption isotherms under ambient conditions (**Figure 3c, d**). CO_2/N_2 (V_{CO2}:V_{N2} = 50:50, 0-1 Bar) IAST selectivity of MIL-125 (Ti_8Ph, 100 °C) (32.2) was around three times higher than that of MIL-125 (TPOT, 150 °C) (11.4), implying that both CO_2 adsorption capacity and CO_2/N_2 adsorption selectivity were positively associated with the missing-linker number in MIL-125 framework, which coincided well with previous research.[17] The fitting curves of CO_2 and N_2 based on the original experimental adsorption data were shown in **Figure S4**, demonstrated that the fitting results of the two molecules are of good accuracy. We therefore concluded that possessing higher missing-linker number in the framework was in favor of enhancing the CO_2/N_2 separation performance of MIL-125 membranes. Moreover, the unary IAST selectivities were plotted by dashed lines in **Figure 3c, d**, calculated based on the unary isotherms (**Figure S3b**), using the partial pressures in the mixture to calculate the loadings. The ratio of the CO_2/N_2 mixture IAST selectivities to unary IAST selectivities for MIL-125 (Ti_8Ph, 100 °C) and MIL-125 (TPOT, 150 °C) were 1.8 and 1.3 at 100 kPa, respectively. In addition, the MIL-125 pore occupancies at 1 bar were less than 10%, therefore, the differences in the IAST selectivities for mixtures and unary selectivities are not large.

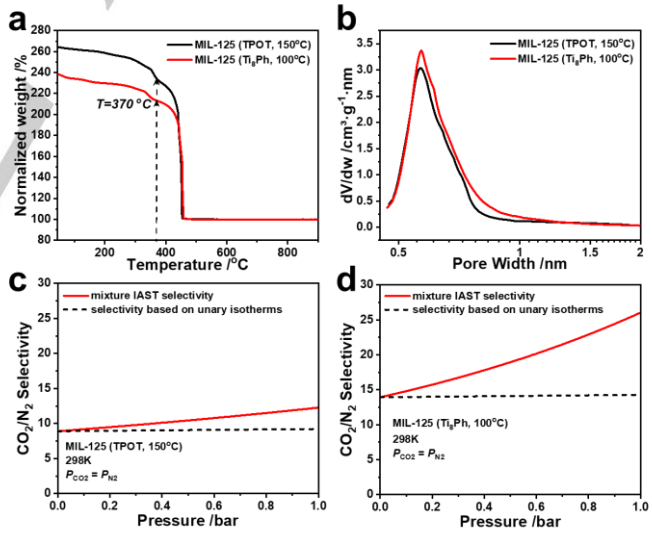

Figure 3. (a) TG curves of MIL-125 (TPOT, 150 °C) and MIL-125 (Ti_8Ph, 100 °C). (b) Pore size distributions of the above samples based on the H-K model. IAST selectivities for mixtures (V_{CO2}:V_{N2} = 50:50, 0-1 bar) and unary selectivities of (c) MIL-125 (TPOT, 150 °C) and (d) MIL-125 (Ti_8Ph, 100 °C).

10.1002/anie.202203663

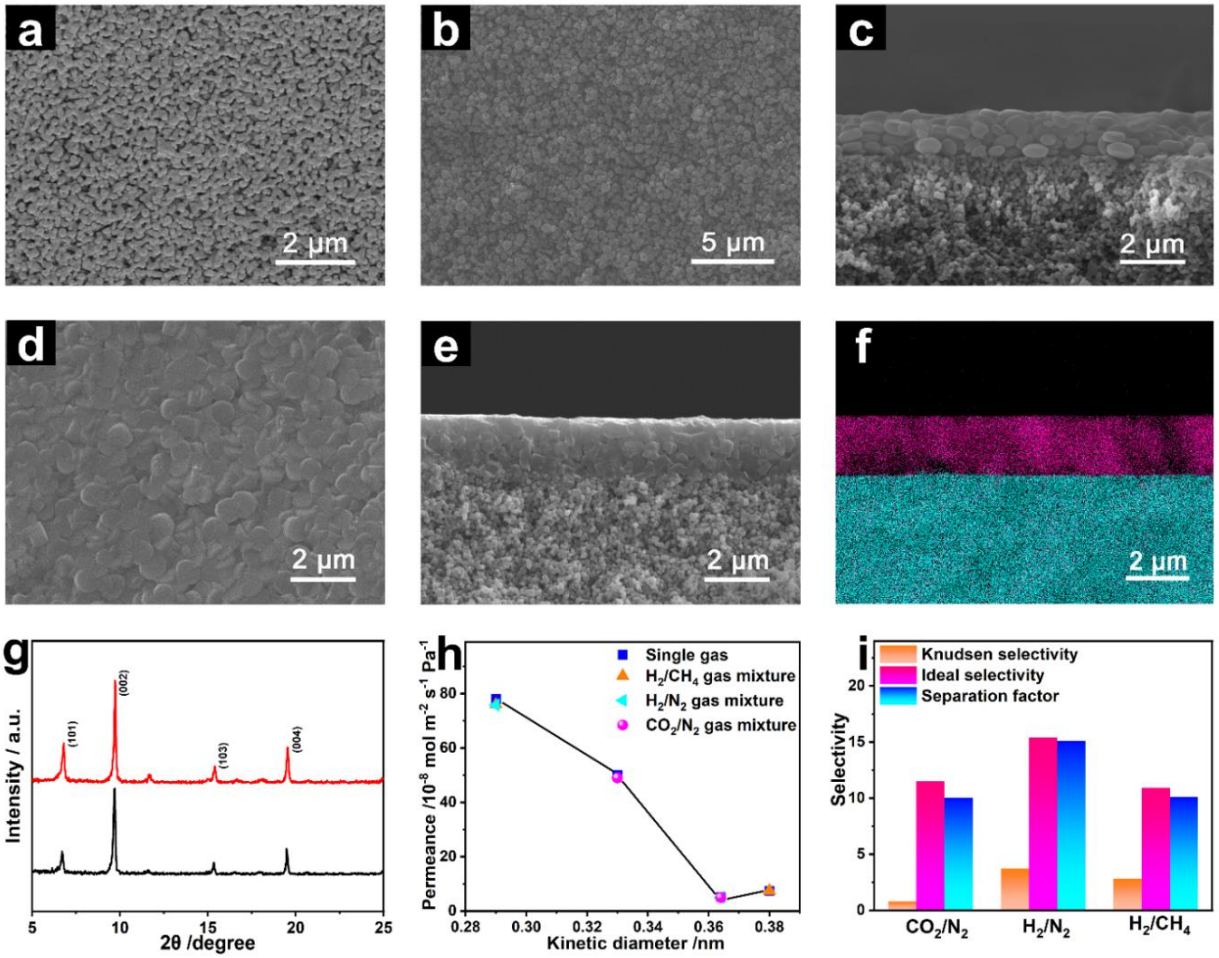

Figure 4. (a) Top SEM image of porous α-Al_2O_3 substrate. Top and cross-sectional SEM images of (b, c) MIL-125 seed layer and (d, e) MIL-125-SG. (f) Cross-sectional EDXS mapping of MIL-125-SG (color code: Ti = red; Al = blue). (g) XRD patterns of MIL-125 seed layer (black line) and MIL-125-SG (red line). (h) Single-gas and mixed-gas permeation properties of MIL-125-SG under ambient conditions. (i) The Knudsen selectivity, ideal selectivity and SF of CO_2/N_2, H_2/N_2, and H_2/CH_4 gas pairs on MIL-125-SG.

Considering the potential impact of temperature on the missing-linker number in MIL-125 framework, herein MIL-125 powders were further synthesized at higher temperatures (120 °C, 140 °C, and 160 °C) using Ti8Ph cluster source. TG results (**Figure S5**) indicated that missing-linker numbers in MIL-125 framework decreased sharply with increasing temperature, resulting in a decrease of both CO_2 adsorption capacity and CO_2/N_2 adsorption selectivity (**Figure S6**). Moreover, the isosteric heats (~21.5 kJ·mol^{-1}) of MIL-125 (Ti_8Ph, 100 °C) were calculated according to the CO_2 adsorption isosteres in a temperature range from 298 to 363 K (**Figure S7**) via the Clausius−Clapeyron equation, which was within the results previously reported in the literature.[18] Therefore, MIL-125 (Ti8Ph, 100 °C), which exhibited the highest missing-linker number and therefore, the highest CO_2 adsorption capacity and CO_2/N_2 adsorption selectivity, were chosen as seeds for the MIL-125 membrane preparation.

Subsequently, the spin-coating technique was employed to deposit MIL-125 (Ti_8Ph, 100 °C) on the porous α-Al_2O_3 substrate. As shown in **Figure 4a, b**, after spin-coating under optimized conditions, a uniform seed layer with thickness of 1.4 μm was obtained. Corresponding XRD pattern indicated that prepared MIL-125 seed layer was preferentially (00l)-oriented.

In the next step, secondary growth was carried out to seal intergranular gaps in the MIL-125 seed layer, during which the Ti_8Ph cluster was served as titanium source and the temperature was kept at 100 °C for maximizing the missing-linker number in the membrane. Relevant SEM images and EDXS pattern (**Figure 4c-e**) indicated that after single-mode microwave heating at 100 °C for 70 min, a well-intergrown MIL-125 membrane with thickness of 1.7 μm was obtained (denoted as MIL-125-SG). Corresponding XRD pattern (**Figure 4f**) confirmed that prepared MIL-125-SG remained preferentially (00l)-oriented. Measurement equipment for single and mixed gas permeation was shown in **Figure S8**. Gas permeation results (**Figure 4g, h** and **Table S1**) indicated that ideal CO_2/N_2, H_2/N_2 and H_2/CH_4 selectivity of the MIL-125-SG reached 11.5, 15.4 and 10.9, respectively, which was much higher than the corresponding Knudsen selectivity (0.8, 3.74 and 2.83, respectively), thereby confirming the existence of few grain boundary defects in the membrane. In addition, prepared membrane maintained high H_2 permeance of 7.8×10^{-7} mol·m^{-2}·s^{-1}·Pa^{-1}.

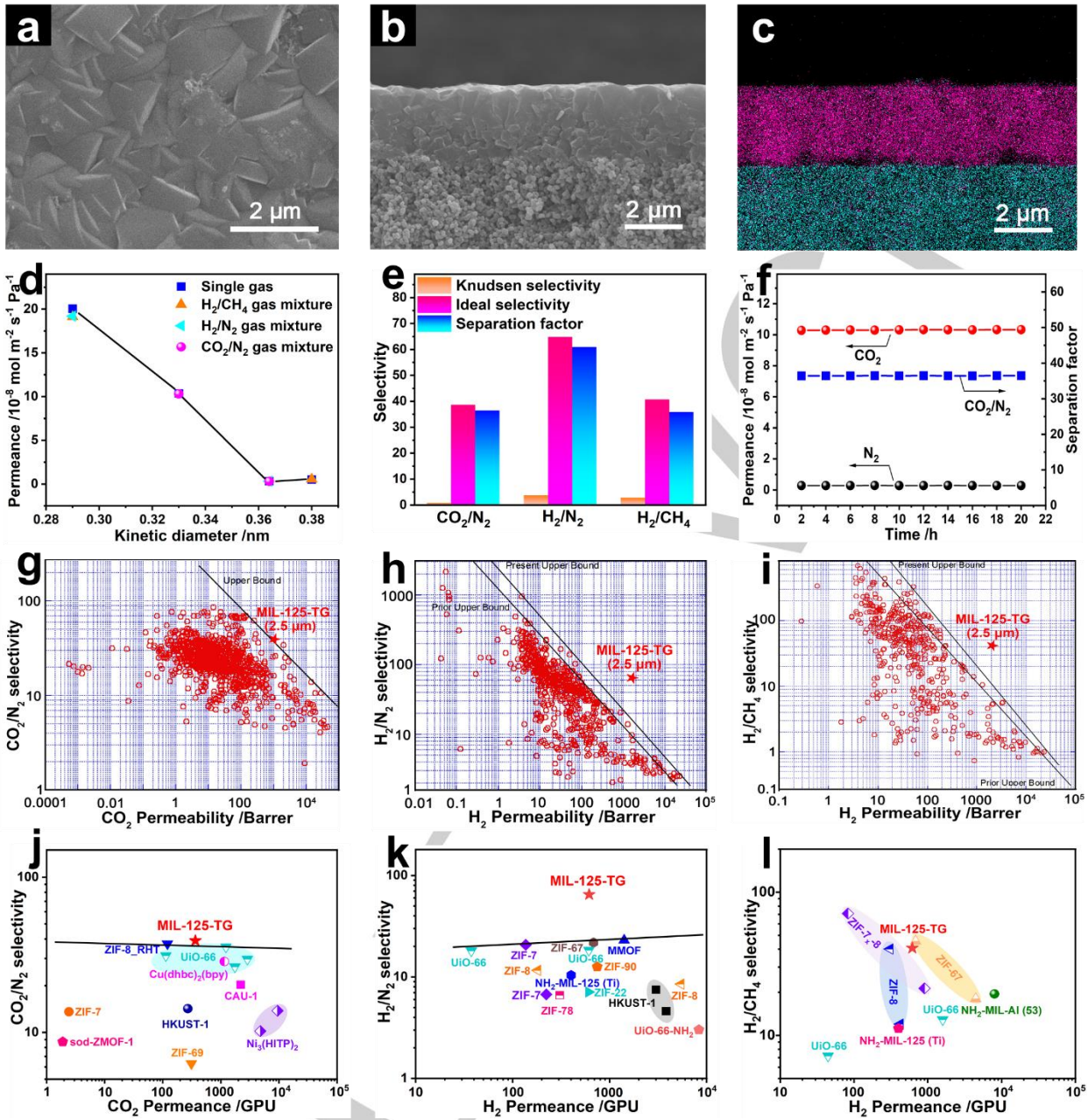

Figure 5. (a) Top and (b) cross-sectional SEM images of MIL-125-TG. (c) Cross-sectional EDXS mapping of MIL-125-TG (color code: Ti = red; Al = blue). (d) Single-gas and mixed-gas permeation properties of MIL-125-TG under ambient conditions. (e) The Knudsen selectivity, ideal selectivity and SF of CO_2/N_2, H_2/N_2 and H_2/CH_4 gas pairs through MIL-125-TG. (f) Long-term stability of MIL-125-TG under ambient conditions. Comparison of (g) CO_2/N_2, (h) H_2/N_2 and (i) H_2/CH_4 separation performances of MIL-125-TG with their respective 2008 Robeson upper bounds. (j) Comparison of CO_2/N_2 separation performance of MIL-125-TG with pristine MOF membranes measured under comparable conditions. Comparison of (k) H_2/N_2 and (l) H_2/CH_4 separation performance of MIL-125-TG with pristine 3D MOF membranes measured under comparable conditions. Detailed data were listed in Table S3-S5.

Afterwards, tertiary growth was carried out to further eliminate grain boundary defects in the membrane. Relevant SEM images (**Figure 5a, b**) showed that prepared MIL-125 membrane (denoted as MIL-125-TG) remained well-intergrown while the thickness was increased to 2.5 μm. Simultaneously, a clear boundary between the MIL-125 top layer and underlying porous α-Al_2O_3 substrate existed in the cross-sectional EDXS pattern (**Figure 5c**), indicating that the formed MIL-125 top layer did not penetrate deep into porous α-Al_2O_3 substrate pores, which was beneficial for reducing the diffusion barrier. Corresponding XRD pattern (**Figure S9**) indicated that prepared MIL-125-TG remained preferentially (00l)-oriented. The dye molecule rejection test was conducted to evaluate whether the grain boundaries are indeed further removed after the tertiary growth. Since the molecular size of congo red (CR) dyes (2.53×0.73 nm) is larger than the pore size of MIL-125 but smaller than that of the grain boundary defect,[19] the CR rejection rate could be a true reflection of the grain boundary defect structure of the corresponding MIL-125 membrane. The dye rejection test results as shown in **Figure S10** indicated that the CR rejection rate of MIL-125-TG reached 99.53%, which was higher than that of MIL-125-SG (98.48%),

which vividly confirmed that majority of grain boundaries were removed after the tertiary growth.

Gas permeation results (**Figure 5d, e** and **Table S2**) indicated that ideal CO_2/N_2, H_2/N_2 and H_2/CH_4 selectivity of prepared MIL-125-TG sharply increased to 38.7, 64.9 and 40.7, respectively, making the overall separation performance well exceeding their respective Robeson 2008 upper bound lines (**Figure 5g-i**).[20] Moreover, according to the sorption-diffusion model, the permeation selectivity (S_{perm}) may be expressed as the product of the adsorption and diffusion selectivities: $S_{perm} = S_{ads} \times S_{diff}$ Since S_{ads} of the CO_2/N_2 gas pair reached 14.3 (based on the IAST theory), correspondingly, the S_{diff} was calculated to be 2.7. Therefore, the excellent CO_2/N_2 separation performance of the MIL-125-TG could be mainly attributed to the high CO_2/N_2 adsorption selectivity.

We further investigated long-term stability of prepared MIL-125-TG (**Figure 5f**). After continuous operation over 20 h, both CO_2 permeance and separation factor (SF) of CO_2/N_2 remained unchanged, which was indicative of excellent operation stability. In particular, the ideal CO_2/N_2 selectivity of the MIL-125-TG was the highest among all pristine polycrystalline MOF membranes (**Figure 5j** and **Table S3**) measured under comparable conditions.[9, 20-21] It should be noted that besides the CO_2/N_2 gas pair, MIL-125-TG membrane also exhibited excellent H_2/N_2 and H_2/CH_4 selectivity. In effect, many literatures have reported microporous materials with relatively large pores but enhancing H_2/N_2 or H_2/CH_4 separations. For instance, Liu et al. prepared well-intergrown, highly c-oriented ultrathin 2D Cu-TCPP (~5.4 Å) membranes on porous α-Al_2O_3 substrates, which displayed H2/CH4 selectivity of ~50[22]; Zhu et al. synthesized large pore (7.5 Å) NH_2-MIL-53 (Al) membranes displaying high SF for H_2/N_2 (23.9) and H_2/CH_4 (20.7) gas mixtures, respectively[23]; Li et al. fabricated UiO-66 (~6.0 Å) membranes with high H_2/N_2 SF (22.4)[21c]; Pinnau et al. prepared AB-type ladder TPIM-1 (~5.5 Å) membranes with high selectivity for H_2/N_2 (~50) and H_2/CH_4 (~53) gas paris[24]; Cooper et al. synthesized porous organic cage (~5.8 Å) membranes displaying the H_2/N_2 selectivity as high as 33[25]. It was highly possible that the unique framework topology of MIL-125 contributed to enhanced H_2/N_2 and H_2/CH_4 separations. In addition, preferred c-orientation, the low reaction temperature and the conduction of tertiary growth were beneficial for reducing grain boundary defects and therefore, enhancing H_2/N_2 and H_2/CH_4 separations of prepared MIL-125 membrane. The ideal H_2/N_2 and H_2/CH_4 selectivity were also superior to most pristine polycrystalline MOF membranes reported in the literature (**Figure 5k, l** and **Table S4, S5**), thereby showing a versatile utility for efficient gas separation on diverse occasions.

Considering its potential applications in industrial separation of CO_2 from flue gases, the CO_2/N_2 separation performance of prepared MIL-125-TG was further studied by simulating the composition of flue gases (V_{CO2}:V_{N2} = 15:85). Gas permeation results indicated that both CO_2 permeance and CO_2/N_2 SF remained largely unchanged (1.1×10^{-7} mol·m^{-2}·s^{-1}·Pa^{-1} and 35.9, respectively), which was in sharp contrast to other CO_2-permselective MOF (e.g., UiO-66 and CAU-1) membranes whose CO_2/N_2 selectivity sharply decreased with decreasing CO_2/N_2 ratio on the feed side [21g, 21h] and therefore, quite advantageous for stable operation under varying working conditions.

Finally, the effect of operating temperature on the CO_2/N_2 separation performance of prepared MIL-125-TG was investigated. As shown in **Figure S11**, the CO_2 permeance first increased with the elevation of temperature and reached maximum value at 90 °C, while further increasing the temperature led to decreased CO_2 permeance. In contrast, the N_2 permeance steadily increased upon elevating temperature, resulting in a steady decrease in SF of CO_2/N_2. To study CO_2 permeation kinetics in the MIL-125 framework in detail, the sorption-diffusion model was employed to investigate the variation trend of adsorption coefficient (S_i) and diffusion coefficient (D_i) for CO_2. The plots of P_{CO2}, D_{CO2}, and, S_{CO2} against temperature were shown in **Figure S12**, which preliminarily proved that CO_2 permeation process was dominantly controlled by diffusion in the case that temperature was lower than 363 K, while it became adsorption-controlled when the temperature became higher than 363 K. Furthermore, we calculated the activation energies of permeability (E_p), heats of adsorption (negative enthalpy of adsorption: -ΔH) and activation energies of diffusion (E_D) for CO_2 (**Table S6**) based on the Arrhenius plots for the permeability, S_{CO2} and D_{CO2} in temperature ranges of 303 to 333 K, 333 to 363 K, 363 to 393 K, and 393 to 423 K (**Figure S13**). To summarize, the above results vividly confirmed that the CO_2 permeability was mainly controlled by diffusion at 303~363 K, while adsorption played a dominant role at 363~423 K.

Considering the potential impact of titanium source on the separation performance of MIL-125 membranes, as a comparative experiment, MIL-125 membranes were further prepared by using 240 nm-sized MIL-125 (TPOT, 150 °C) (**Figure S14a**) as seeds and TPOT as titanium source during membrane growth while keeping other synthetic conditions unchanged. Our experimental results indicated that even after tertiary growth at 100 °C for 70 min, prepared MIL-125 membrane remained poorly intergrown (**Figure S14b-e)**, which might be attributed to relatively high activation energy required for the $Ti_8(\mu_2\text{-}O)_8(\mu_2\text{-}OH)_4$ node formation before the membrane growth. As a result, elevating the temperature to 160 °C was indispensable for the well intergrowth between adjacent MIL-125 crystallites (**Figure S15**).[5, 26] Gas permeation results indicated that ideal CO_2/N_2, H_2/N_2 and H_2/CH_4 selectivity of the MIL-125 membrane synthesized at 160 °C was only 5.3, 7.0 and 1.5 (**Table S7 and S8**), which could be ascribed to relatively low missing-linker number (~0.4) in the membrane, resulting in lower CO_2/N_2 adsorption selectivity and therefore, inferior CO_2/N_2 separation performance.

To investigate the impact of heating mode on the separation performance, MIL-125 membranes were further prepared by convective heating for comparison. As shown in **Figure S16**, substantial voids and cracks remained visible in the membrane even after prolonged growth (24 h). Simultaneously, we observed that substantial MIL-125 particles (mass: 90 mg, yield: 92%) were spontaneously formed and sedimented to the bottom of the vessel after the reaction (**Figure S17**). Accordingly, failure of well-intergrown MIL-125 membrane formation could be ascribed to excessive MIL-125 nucleation and growth in the bulk solution, resulting in over-consumption of nutrients there and therefore, inadequate nutrient supply for sealing intergranular gaps in the membrane. In contrast, owing to the nucleation bottleneck effect, only a small amount of amorphous powders was generated in the bulk solution in the case of single-mode microwave heating, resulting in effective suppression of MIL-125 nucleation in the bulk solution and therefore, sufficient nutrient supply for the formation of well-intergrown MIL-125 membranes.[5, 26]

To investigate the influence of reaction temperature on the separation performance, MIL-125 membranes were further

prepared at 160 ºC with Ti_8Ph cluster source while keeping other reaction conditions unchanged. SEM results (**Figure S18**) indicated that after tertiary growth, a well-intergrown, 3.8 μm-thick MIL-125 membrane was obtained. Gas permeation results indicated that ideal CO_2/N_2, H_2/N_2 and H_2/CH_4 selectivity of the membrane was 9.0, 8.3 and 5.2, respectively (**Table S9**). The relatively low selectivity could be attributed to effective elimination of missing-linker defects (missing-linker number: 0) in the framework at such a high temperature, resulting in lower CO_2/N_2 adsorption selectivity.

Conclusion

With Ti_8Ph cluster as titanium source, high defective MIL-125 membrane was successfully fabricated through combining single-mode microwave heating with tertiary growth in this study. Employing Ti_8Ph cluster source led to not only a lower reaction temperature required for the formation of well-intergrown MIL-125 membrane but also a higher missing-linker number within the framework, resulting in enhanced CO_2/N_2 adsorption selectivity. Prepared MIL-125 membrane exhibited an ideal CO_2/N_2 selectivity of 38.7, which ranked the highest among all pristine polycrystalline MOF membranes measured under similar conditions. Of particular note, simulated flue gas separation experiment indicated that both CO_2 permeance and CO_2/N_2 SF (35.9) remained unchanged, which was in sharp contrast to other CO_2-permselective MOF membranes whose CO_2/N_2 selectivity sharply decreased with decreasing CO_2/N_2 ratio on the feed side, which was quite advantageous for stable operation under varying working conditions. In addition, its ideal H_2/N_2 and H_2/CH_4 selectivity (64.9 and 40.7) were considerably high. It is anticipated that the concept of using metal-oxo clusters as metal sources could bring new insights into diverse high-performance MOF membrane preparations.

Acknowledgments

We are grateful to National Natural Science Foundation of China (22078039, 21922810), Science and Technology Innovation Fund of Dalian (2020JJ26GX026), Fok Ying-Tong Education Foundation of China (171063), Science Fund for Creative Research Groups of the National Natural Science Foundation of China (22021005), National Key Research and Development Program of China (2019YFE0119200), and the Technology Innovation Team of Dalian University of Technology (DUT2017TB01) for the financial support.

Keywords: gas separation • Ti-oxo cluster • membrane • structural defects • metal-organic frameworks (MOFs)

[1] S. Hong, Y. Jeong, H. Baik, N. Choi, A. C. K. Yip, J. Choi, *Angew. Chem. Int. Ed.* **2021**, *60*, 1323-1331.

[2] a) M. Dan-Hardi, C. Serre, T. Frot, L. Rozes, G. Maurin, C. Sanchez, G. Férey, *J. Am. Chem. Soc.* **2009**, *131*, 10857-10859; b) S. Yang, L. Peng, S. Bulut, W. L. Queen, *Chem. Eur. J.* **2019**, 25, 2161-2178.

[3] a) Y. Sun, D.-F. Lu, Y. Sun, M.-Y. Gao, N. Zheng, C. Gu, F. Wang, J. Zhang, *ACS Mater. Lett.* **2020**, *3*, 64-68; b) P. Ji, Y. Song, T. Drake, S. S. Veroneau, Z. Lin, X. Pan, W. Lin, *J. Am. Chem. Soc.* **2018**, *140*, 433-440.

[4] S. Friebe, A. Mundstock, D. Unruh, F. Renz, J. Caro, *J. Membr. Sci.* **2016**, *516*, 185-193.

[5] Y. Sun, Y. Liu, J. Caro, X. Guo, C. Song, Y. Liu, *Angew. Chem. Int. Ed. Engl.* **2018**, *57*, 16088-16093.

[6] H. Assi, G. Mouchaham, N. Steunou, T. Devic, C. Serre, *Chem. Soc. Rev.* **2017**, *46*, 3431-3452.

[7] Z. Qiao, Y. Liang, Z. Zhang, D. Mei, Z. Wang, M. D. Guiver, C. Zhong, *Adv. Mater.* **2020**, *32*, e2002165.

[8] T. H. Lee, J. G. Jung, Y. J. Kim, J. S. Roh, H. W. Yoon, B. S. Ghanem, H. W. Kim, Y. H. Cho, I. Pinnau, H. B. Park, *Angew. Chem. Int. Ed. Engl.* **2021**, *60*, 13081-13088.

[9] J. Yan, Y. Sun, T. Ji, L. Liu, M. Zhang, Y. Liu, *J. Membr. Sci.* **2021**, *635*, 119515.

[10] a) V. Guillerm, S. Gross, C. Serre, T. Devic, M. Bauer, G. Ferey, *Chem. Commun.* **2010**, *46*, 767-769; b) D. C. Oliveira, A. G. Macedo, N. J. O. Silva, C. Molina, R. A. S. Ferreira, P. S. Andre, K. Dahmouche, V. D. Z. Bermudez, Y. Messaddeq, S. J. L. Ribeiro, L. D. Carlos, *Chem. Mater.* **2008**, *20*, 3696-3705.

[11] Y. Keum, S. Park, Y.-P. Chen, J. Park, *Angew. Chem. Int. Ed.* **2018**, *57*, 14852-14856.

[12] S. Wang, H. Reinsch, N. Heymans, M. Wahiduzzaman, C. Martineau-Corcos, G. De Weireld, G. Maurin, C. Serre, *Matter* **2020**, *2*, 440-450.

[13] S. Hu, M. Liu, X. Guo, K. Li, Y. Han, C. Song, G. Zhang, Cryst. Growth Des. **2017**, *17*, 6586-6595.

[14] T. Frot, S. Cochet, G. Laurent, C. Sassoye, M. Popall, C. Sanchez, L. Rozes, *Eur. J. Inorg. Chem.* **2010**, *2010*, 5650-5659.

[15] G. C. Shearer, S. Chavan, S. Bordiga, S. Svelle, U. Olsbye, K. P. Lillerud, *Chem. Mater.* **2016**, *28*, 3749-3761.

[16] Ü. Kökçam-Demir, A. Goldman, L. Esrafili, M. Gharib, A. Morsali, O. Weingart, C. Janiak, *Chem. Soc. Rev.* **2020**, *49*, 2751-2798.

[17] J. N. Hall, P. Bollini, *React. Chem. Eng.* **2019**, *4*, 207-222.

[18] S.-N. Kim, J. Kim, H.-Y. Kim, H.-Y. Cho, W.-S. Ahn, *Catal.Today* **2013**, 204, 85-93.

[19] S. Hong, D. Kim, H. Richter, J.-H. Moon, N. Choi, J. Nam, J. Choi, *J. Membr. Sci.* **2019**, 569, 91-103.

[20] L. M. Robeson, *J. Membr. Sci.* **2008**, *320*, 390-400.

[21] a) B. A. Al-Maythalony, O. Shekhah, R. Swaidan, Y. Belmabkhout, I. Pinnau, M. Eddaoudi, *J. Am. Chem. Soc.* **2015**, *137*, 1754-1757; b) D. S. Chiou, H. J. Yu, T. H. Hung, Q. Lyu, C. K. Chang, J. S. Lee, L. C. Lin, D. Y. Kang, *Adv. Funct. Mater.* **2020**, *31*, *2006924*; c) X. Liu, N. K. Demir, Z. Wu, K. Li, *J. Am. Chem. Soc* **2015**, *137*, 6999-7002; d) Y. Liu, G. Zeng, Y. Pan, Z. Lai, *J. Membr. Sci.* **2011**, *379*, 46-51; e) R. Rong, Y. Sun, T. Ji, Y. Liu, *J. Membr. Sci.* **2020**, *610*, 118275; f) M. N. Shah, M. A. Gonzalez, M. C. McCarthy, H.-K. Jeong, *Langmuir* **2013**, *29*, 7896-7902; g) W. Wu, Z. Li, Y. Chen, W. Li, Environ. Sci. Technol. **2019**, *53*, 3764-3772; h) H. Yin, J. Wang, Z. Xie, J. Yang, J. Bai, J. Lu, Y. Zhang, D. Yin, J. Y. Lin, *Chem. Commun. (Camb)* **2014**, *50*, 3699-3701; i) R. W. Baker, B. T. Low, *Macromolecules* **2014**, *47*, 6999-7013; j) M. Galizia, W. S. Chi, Z. P. Smith, T. C. Merkel, R. W. Baker, B. D. Freeman, *Macromolecules* **2017**, *50*, 7809-7843; k) T. H. Lee, A. Ozcan, I. Park, D. Fan, J. K. Jang, P. G. M. Mileo, S. Y. Yoo, J. S. Roh, J. H. Kang, B. K. Lee, Y. H. Cho, R. Semino, H. W. Kim, G. Maurin, H. B. Park, *Adv. Funct. Mater.* **2021**, *31*, *2103973*; l) U. W. R. Siagian, A. Raksajati, N. F. Himma, K. Khoiruddin, I. G. Wenten, *J. Nat. Gas Sci. Eng.* **2019**, *67*, 172-195; m) Y. Wang, H. Jin, Q. Ma, K. Mo, H. Mao, A. Feldhoff, X. Cao, Y. Li, F. Pan, Z. Jiang, *Angew. Chem. Int. Ed. Engl.* **2020**, *59*, 4365-4369; n) S. Jiang, X. Shi, F. Sun, G. Zhu, *Chem. Asian J.* **2020**, *15*, 2371-2378; o) S. Jiang, X. Shi, Y. Zu, F. Sun, G. Zhu, *Mater. Chem. Front.* **2021**, *5*, 5150-5157; p) Y. Ying, Z. Zhang, S. B. Peh, A. Karmakar, Y. Cheng, J. Zhang, L. Xi, C. Boothroyd, Y. M. Lam, C. Zhong, D. Zhao, *Angew. Chem. Int. Ed.* **2021**, *60*, 11318-11325.

[22] Y. Song, Y. Sun, D. Du, M. Zhang, Y. Liu, L. Liu, T. Ji, G. He, Y. Liu, *J. Membr. Sci.* **2021**, 634, 119393.

[23] F. Zhang, X. Zou, X. Gao, S. Fan, F. Sun, H. Ren, G. Zhu, *Adv. Funct. Mater*. **2012**, 22, 3583-3590.

[24] B. S. Ghanem, R. Swaidan, X. Ma, E. Litwiller, I. Pinnau, *Adv.Mater.* **2014**, 26, 6696-6700.

[25] Q. Song, S. Jiang, T. Hasell, M. Liu, S. Sun, A. K. Cheetham, E. Sivaniah, A. I. Cooper, *Adv.Mater*. **2016**, 28, 2629-2637.

[26] Y. Sun, C. Song, X. Guo, S. Hong, J. Choi, Y. Liu, *J. Membr. Sci*. **2020**, 616, 118615.

10.1002/anie.202203663

WILEY-VCH

RESEARCH ARTICLE

Entry for the Table of Contents

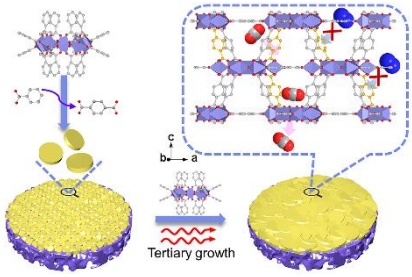

With the titanium-oxo cluster $Ti_8(\mu_2\text{-}O)_8(OOCC_6H_5)_{16}$ as the titanium source, a MIL-125 metal-organic framework (MOF) membrane was prepared under mild reaction conditions through combining single-mode microwave heating with tertiary growth. Using this titanium source and maintaining a lower reaction temperature increased the missing-linker number in the MIL-125 framework and therefore enhanced the CO_2/N_2 selectivity.